Contents lists available at ScienceDirect

Toxicology Reports

Peripheral serum iTRAQ-based proteomic characteristics of carbon tetrachloride-induced acute liver injury in *Macaca fascicularis*

Miao Yufa [a,1], Chen Dongmei [b,1], Li Wei [a], Li Shuangxing [a], Sun Li [a], Geng Xingchao [a,*]

[a] *National Center for Safety Evaluation of Drugs, National Institutes for Food and Drug Control, Beijing Key Laboratory for Safety Evaluation of Drugs, Beijing 100176, China*
[b] *Beijing Red Cross Blood Center, Beijing 100088, China*

ARTICLE INFO

ABSTRACT

Carbon tetrachloride (CCl_4) is a potent chemical compound that can induce liver cells necrosis. The purpose of this study was to evaluate the hepatic toxicity of CCl_4 exposure in *Macaca fascicularis* to explore the liver toxicity mechanism using a proteomic approach. One animal (no.F6) was intoxicated by oral gavage with 15 % CCl_4 solution (10 mL/kg, dissolved in edible peanut oil), and was sacrificed at 48 h after CCl_4 administration. Another blank control animal (no.F4) was sacrificed at the same time. The liver cells of the blank control animal showed normal hepatocyte morphology. However, the hepatocytes at 48 h time point after CCl_4 administration showed necrosis and vacuolation histopathologically. The animal No.F7~F12 and no.M7~M12 were administrated by gavage with 15 % CCl_4 solution (10 mL/kg, dissolved in edible peanut oil). Blood samples were collected before gavage administration, and served as the 0 h blank control samples. Then, blood samples were collected at 2 h, 48 h, 72 h and 168 h after CCl_4 exposure, and served as the test samples. Routine biochemistry and immunical parameters were performed using biochemistry analyzer for all serum. Then the serum from male and female animals at 0 h, 2 h, 48 h, and 72 h was mixed, respectively. The peripheral serum proteins at 0 h, 2 h, 48 h, and 72 h were extracted, then the proteins were enzymatically hydrolyzed and the peptides were isotopic labeled by isobaric tags for relative and absolute quantification (iTRAQ). Finally, the UniProt Protein Sequence Library of *Macaca fascicularis* was queried to identify and compare the differential proteins between different time points. The results showed that, as traditional biomarkers of liver injury, alanine aminotransferases (ALT) and aspartate aminotransferases (AST) showed a typical time-effect curve. Compared with 0 h, there were totally 55, 323, and 158 differential proteins (*P* value <0.05, Ratio fold >1.5, FDR<0.05) at 2 h, 48 h and 72 h, respectively. GO enrichment analysis of differentially expressed proteins only at 48 h involved 3 cellular components (*P* adjust value <0.05), and differential proteins at other time points had no significant enrichment. Furthermore, KEGG enrichment analysis showed that the toxicity effect of CCl_4 at different time points after administration was mediated through 22 pathways such as biosynthesis of antibiotics, carbon metabolism, biosynthesis of amino acids, peroxisome, cysteine and methionine metabolism, arginine biosynthesis, and complement and coagulation cascades (*P* adjust value <0.05). Among them, the counts of signaling pathway involved biosynthesis of antibiotics, carbon metabolism and biosynthesis of amino acids were more than 10 and the three pathways may play a greater role in toxicity progress after administration of CCl_4. PPI network analysis showed that there were 3, 52, and 13 nodes in the interaction of differential proteins at 2 h, 48 h, and 72 h, respectively. In conclusion, many differential proteins in peripheral blood were detected after CCl_4 administration, and the GO and KEGG enrichment analysis showed the toxicological mechanisms of CCl_4-induced liver injury and potential protection reaction mechanism for CCl_4 detoxication may be related with multi biological processes, signaling pathway and targets.

1. Introduction

CCl$_4$-induced acute liver injury in animal models was widely used to deeply investigate the liver toxicity mechanism. CCl$_4$ exposure has many flexible approaches, which can be administrated intraperitoneally, by inhalation, and through an orogastric or nasogastric tube [1]. In a previous study, Sprague-Dawley rats were injected with intraperitoneal treatment of 1 mL/kg bw of CCl$_4$ diluted with olive oil (CCl$_4$: olive oil; 3:7 v/v) thrice a week on alternate days to induce hepatotoxicity. The treatment with CCl$_4$ significantly increased the level of alkaline phosphatase (ALP), ALT, AST and total bilirubin (TBIL). On the other hand, a notable decline in albumin (ALB) concentration was observed [2]. For CCl$_4$-induced liver injury in mice, the animals were injected with CCl$_4$ (15 mL/kg; i.p.) dissolved in olive oil (CCl$_4$: olive oil; 1:3 v/v). The results showed that the serum activities of ALT and AST increased in the CCl$_4$ group compared with the blank control group, and the liver malondialdehyde (MDA) amount and liver glutathione (GSH) level increased significantly in the CCl$_4$-treated mice. The mice in the CCl$_4$ group showed serious liver damage, indicated by obvious hepatocyte necrosis and shrinkage nuclei. Moreover, the liver mRNA expressions of Prx 1–3, 5, 6, Trx1/2 and TrxR1/2, HO-1 and Nrf2 in CCl$_4$-treated mice all decreased remarkably compared with the control group [3]. Generally, CCl$_4$ is considered to be metabolized by the cytochrome P450 enzymes to form reactive intermediates, such as trichloromethyl-free radicals and peroxyl radical, which then initiate lipid peroxidation, cellular damage and liver fibrosis. However, the toxicological mechanisms remain not fully understood and need to be explored deeply.

Macaca fascicularis, also referred to as cynomolgus monkey, comprises 9 subspecies and naturally occurred in Southeast Asia, such as Indonesia, Vietnam and Philippines. Since the 17th century, *Macaca fascicularis* also occurs on Mauritius. Because of its small size, long tail, mild-mannered personality, short reproductive cycle and lack of seasonal defects, it became one of the most predominant nonhuman primate animal models in basic and applied biomedical research. Moreover, using a whole-genome shotgun sequencing, the 17,387 orthologs of human protein-coding genes in the Mauritian *Macaca fascicularis* draft genome were identified. So it was considered that the primate experiments had good predictive power for human [4]. Animals from different countries within Asia mainland do not appear to show any meaningful difference. Very little data is available for animals from Asia island. Mauritian animals show consistent differences from Asian animals in several clinical and anatomical pathology parameters. In this study, *Macaca fascicularis* bred in China were considered to have similar genome to Mauritian animals, and have good predictive ability for human [5].

Isobaric tag for relative and absolute quantitation (iTRAQ) technique is a polypeptide labeling technique in vitro developed by Applied Biosystems Incorporation in 2004. Four or eight isotope tags were used to label specific amino acid sites of peptide segments, and then tandem mass spectrometry analysis was performed to compare the differentially expressed proteins of 2–8 groups of samples in the meantime [6]. Gene Ontology (GO) is a database established by the Association for Gene Ontology that is applicable to species and that defines and describes the functions of genes and proteins. Using the GO database, genes can be classified according to the biological processes they participate in, the components that make up cells, and the molecular functions they perform. So the GO annotation makes it easier for us to understand the biological meaning behind the genes [7]. KEGG is the Kyoto Encyclopedia of Genes and Genomes Database. KEGG pathway analysis of identified proteins can enhance the understanding of metabolic capacity, biological information processes and related diseases [8]. Proteins usually perform biological functions synergistically. Using the String protein-protein interaction database, Protein-Protein interaction (PPI) network analysis of significantly different expressed proteins could be performed. Strong relationships have been shown to exist between the biological functions of protein clusters and PPIs. PPI network analysis is helpful for finding hub proteins among a cluster of differential proteins based on their interaction levels [9].

Proteomics is a comprehensive proteins study, including information on protein abundance and modification, along with their interaction networks. Studies of liver injury have been limited to rodent models on the transcriptomic or proteomics level, and according to the results of PubMed search using keywords *Macaca fascicularis*, proteomics, and hepatotoxicity, no relevant literature was found. More important, hepatotoxicity studies in primate models will be closer to human liver injury. Based on this consideration, the objectives of the present study are to find out the differential proteins in the serum of *Macaca fascicularis* after CCl$_4$ administration, and explore the liver toxicity mechanism of CCl$_4$ through GO enrichment analysis, KEGG analysis, and PPI analysis, as well as identify potential therapeutic targets.

2. Material and methods

2.1. Animals and equipments

Fourteen 3-year-old *Macaca fascicularis*, 6 male (animal No. M7~M12) and 8 female (animal No.F4,F6,F7~F12), normal grade, weight 2.25–3.90 kg, were purchased from Guangxi Guidong Primate Development and Experiment Co., Ltd [production license: SCXK (Guangxi Zhuang Autonomous Region) 2022–0003]. The animals were reared in the Animal Room No.10 of National Center for Safety Evaluation of Drugs (NCSED) [license for animal use: SYXK (Beijing) 2021–0072] according to the good laboratory practice (GLP) of the People's Republic of China (Order No. 34 of CFDA , 2017). The institute was accredited by the Association for Assessment and Accreditation of Laboratory Animal Care International (AAALAC) and the study was approved by Institutional Animal Care and Use Committee (IACUC) of the center with approval number IACUC-2019-K007. The clinical pathology laboratory of NCSED was firstly accredited by the College of American Pathologists (CAP, Illinois, USA) in 2010, and thereafter obtained reaccreditation every two years, and kept being accreditated until now. The experimenters were trained and certified to work with experimental animals to assure that the "3 R" principle in the research process was followed, and that the experimental animals were given the necessary welfare and care.

2.2. Reagents

CCl$_4$ (analytically purity) was purchased from Beijing Chemical Plant (Beijing, China). Trypsin was obtained from Promega (Madison, Wisconsin, USA). Coomassie Brilliant Blue dye G250 was supplied by Amresco (Ladner, Pennsylvania, USA). Acrylamide and SDS were acquired from Sigma -Aldrich (St. Louis, MO, USA). Acetonitrile and methanol were obtained from Thermo Fisher (Waltham, Massachusetts, USA). Strata-x C18 desalination column and SCX strong cation exchange column were purchased from Phenomenex (Los Angeles, California, USA). iTRAQ Reagent 8-Plex Multiplex kit was supplied by AB SCIEX (San Jose, California, USA). Serum protein extraction Kit was purchased from Epigentek (Farmingdale, NY, USA). All biochemical parameters kits were supplied by Wako (Tokyo, Japan). The other reagents were all made in China.

2.3. In vivo experimental design

The animal No.F4 was the blank control animal, which received nothing administration. The animal No.F6 was the positive control animal, which was intoxicated by oral gavage with 15 % CCl$_4$ solution (10 mL/kg, dissolved in edible peanut oil). Oral dose design was carried out according to the literature reported by Binitha, R. R. V and Lee, I. C [10,11]. The time point before gavage administration was defined as 0 hours. The positive control animal was sacrificed at 48 h after administration and the blank control animal was sacrificed at the same

time. Euthanasia was carried out by intravenous injection of 3.5 % sodium pentobarbital at an anesthetic dose of 35 mg/kg. The volume of the anesthetic was calculated according to the results of the recent body weight weighing. Liver tissues were collected from F4 and F6, and fixed in 4 % formalin solution for 48 h. The tissues were dewaxed in xylene and rehydrated in a series of graded alcohols and then embedded in paraffin. The liver tissues were sectioned at 4 μm and stained with HE (hematoxylin and eosin) for pathological microscope examination [12].

The animal No.F7~F12 and M7~M12 were also administrated by gavage with 15 % CCl₄ solution (10 mL/kg, dissolved in edible peanut oil). Peripheral blood samples were collected before gavage administration, and served as the 0 h blank control samples. Then, peripheral blood samples were collected at 2 h, 4 h, 24 h, 48 h, 72 h, and 168 h after CCl₄ exposure, and served as the test samples. All blood samples were obtained from the forearm vein after fasting overnight. The volume of all samples was approximately 1.5 mL , and the vacuum blood collection tubes were used with no anticoagulant. All blood samples were stored at room temperature for no less than 30 min and were centrifuged at a speed of 3000 r/min for 10 min to prepare serum. Biochemical analysis of all serum was performed. Serum from male and female animals at 0 h, 2 h, 48 h, and 72 h was mixed separately, and the all mixed serum at different time points was used for protein extraction and mass spectrometry identification.

2.4. Biochemical analysis

The biochemical indicators including alanine aminotransferase (ALT), aspartate aminotransferase (AST), ALP, gamma-glutamic acyl-transferase (GGT), creatine phosphokinase (CK), lactic dehydrogenase (LDH), TBIL, urea (UREA), creatinine (CRE), glucose (GLU), cholesterol (CHO), triglycerides (TG), total protein (TP), ALB, calcium (Ca), inorganic phosphorus (P), sodium (Na$^+$), potassium (K$^+$), chloride (Cl$^-$) and five immunological indexes (IgG, IgA, IgM, C3, and C4) were quantified using HITACHI 7180 automatic biochemistry analyzer (Tokyo, Japan) in NCSED. Internal quality control was performed before and after each day of experiments, and external quality assessment was performed using samples from College of American Pathologists (CAP, Illinois, USA) every four months. Results for each biochemical indicators included results of six females and six males. Data was expressed as the means ±SEM for each time point and was analyzed using the statistical package IBM SPSS Statistics 19.0 version software. To compare values obtained from different time points, the Student 's t test was performed. P values of < 0.05 were considered significant.

2.5. Protein preparation and iTRAQ labeling

The Aurum™ Serum Protein Mini Kit (Bio-Rad) was employed to extract proteins and reduce the high-abundance proteins influence according to the manufacturer's instruction. Briefly, the serum was centrifuged at 16,000 r/min for 5 min and the precipitate was discarded. The samples were mixed with the serum protein binding buffer in a 1:3 ratio. Then diluted serum was added to well-prepared column. The column was gently vortexed and repeated every 5–10 min for 2 times. The column was placed in a new centrifuge tube for 2 min and centrifuged at 10,000 g for 20 s to collect the solution. A 200 μl binding buffer was added to the column and centrifuged at 10,000 g for 20 s to collect the solution. The two solutions were mixed. Four times the volume of ice pre-cooled acetone (containing 0.07 % beta-mercaptoethanol) was added to precipitate overnight. Then, the solution was centrifugated at 10,000 g, and the precipitate was cleaned with ice pre-cooling acetone (containing 0.07 % beta-mercaptoethanol) for 3 times. The protein solution dissolved by 200 μl lysis buffer was used for SDS-PAGE and to determine the protein concentration through a Bradford protein assay.

Protein digestion was conducted according to the FASP procedure as a previous description [13]. In brief, for each sample, 100 μg of proteins were solubilized in 10 μl Reducing Reagent at 37 °C for 60 min. Then 2 μl

Cysteine-Blocking Reagent was added at room temperature for 30 min. The protein solution was transferred into a 10 kd centrifugal ultrafiltration units and centrifugated at 12,000 g for 20 min. The filters were washed with 100 μl of Dissolution Buffer (Applied Biosystems, Foster City, CA, USA) and centrifuged at 12,000 g for 20 min, which was repeated three times. Proteins were then in-solution digested with trypsin according to the protein/trypsin ratio of 50:1 at 37 °C overnight. Morrow, the filter unit was transferred to a new tube and centrifuged at 12,000 g for 15 min. The filtrate was collected and the peptide concentration was estimated by UV light spectral density at 280 nm.

Labeling of the peptides was performed using an iTRAQ Reagent 8-Plex Multiplex kit according to the manufacturer's protocol. In the present iTRAQ measurements, equal amount of 12 biological replicates at different time points were mixed to produce a sample pool. After that, each sample was labeled with a different iTRAQ tag as follows: 0 h blank control, tag 113 and 114; 2 h after CCl₄ treatment, tag 115 and 116; 48 h after CCl₄ treatment, tag 117 and 118; 72 h after CCl₄ treatment, tag 119 and 121. All of the iTRAQ labeled samples were then pooled and dried using a vacuum dryer. An experimental workflow for protein profiling and sample labeling were shown in Fig. 1 and Table 1.

2.6. Reverse-phase (RP) HPLC

The labeled peptide fragments of each sample were reconstituted with 100 μl buffer A (98 % ddH₂O, 2 % acetonitrile, pH 10) followed by centrifugation at 14,000 r/m for 10 min and then eluted with a gradient buffer B (98 % acetonitrile, 2 % ddH2O, pH 10) using RIGOL L-3000 high performance liquid chromatography system (Beijing RIGOL Technology Co., Ltd., Beijing, China) with an RP analytical column (Durashell-C18, 4.6 mm × 250 mm, 5 μ m, 100 Å) at a flow rate of 700 μl/min. Fractions were collected and all samples were stored at −80℃ before LC-MS/MS analysis.
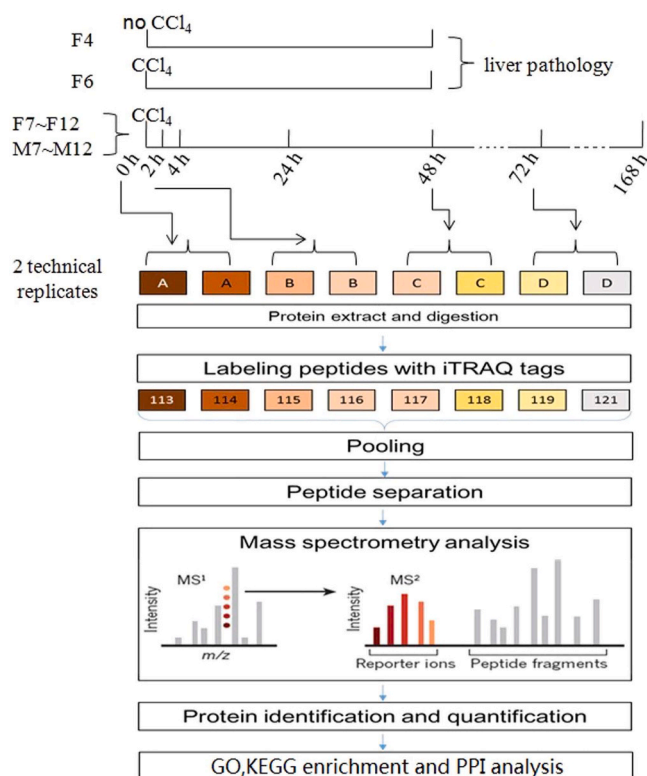

Fig. 1. An experimental workflow for protein profiling.

Table 1
Samples design for iTRAQ experiment.

Code No.	Samples at different time points	Tag No.	Comparison of samples	Ratio
A	0 h	113	-	-
A	0 h	114	-	-
B	2 h	115	2 h vs. 0 h	115/113,115/114
B	2 h	116	2 h vs. 0 h	116/113,116/114
C	48 h	117	48 h vs. 0 h	117/113,117/114
C	48 h	118	48 h vs. 0 h	118/113,118/114
D	72 h	119	72 h vs. 0 h	119/113,119/114
D	72 h	121	72 h vs. 0 h	121/113,121/114

Note: Sample at each time point represents a mixture of six females and six males. Time points represent samples from different time points.

2.7. LC-MS/MS analysis

The peptide fragments from each sample were redissolved in 2 % methyl alcohol and 0.1 % formic acid and then centrifuged at 13,000 r/min for 10 min. The LC-MS/MS was performed using Easy-nLC nanoflow HPLC system connected to Q Exactive mass spectrometer (Thermo Fisher Scientific, San Jose, CA, USA). MS spectra were acquired over a range of 350–1800 m/z, and resolving powers of the MS scan and MS/MS scan at 200 m/z were set as 70,000 and 17,500, respectively. Each sample was loaded onto Acclaim PepMap 100 C18 (2 cm × 100 μm, 5 μm C18) using an autosampler and then the sequential separation of peptides on Thermo Scientific EASY column (EASY-Spray column, 12 cm × 75 μm, C18, 3 μm) was accomplished with a gradient of buffer B (100 % acetonitrile and 0.1 % formic acid) at a flow rate of 350 nl/min.

2.8. Differential proteins analysis

The raw data was analyzed using the Proteome Discoverer 1.4 software (Thermo Fisher Scientific, USA) to identify the proteins in a search of the protein database of *Macaca fascicularis* downloaded from National Center for Biotechnology Information (NCBI, http://www.ncbi.nlm.nih.gov/) (download date August 7, 2020). For protein identification, the following search parameters were as follows: Precursor ion mass tolerance ±15 ppm; MS/MS tolerance ± 0.1 Da; 2 missed cleavages were allowed with the enzyme of trypsin; cysteine was set as fixed modification of carbamidomethylation (C) and methionine (M) was set as variable modifications of oxidation. Spectrum mill determines the area for each precursor and, following peptide spectral matching, assigns the peak area to the corresponding peptide. Protein intensity was calculated as the median intensity of the peptides from the protein. Under the condition of repeated experiment, the *t*-test was used to screen the differentially expressed proteins according to the comparison of repeated markers in each sample. *P* value < 0.05 was considered statistically significant. The proteins with a false discovery rate (FDR) less than 0.05 and the fold of difference greater than 1.5 were the significant difference proteins. The proteins with ratio more than 1.5 were the significantly up-regulated proteins, and the proteins with ratio less than 0.67 (1/1.5) was the significantly down-regulated proteins [14].

2.9. Genome ontology (GO) enrichment analysis

GO is a database established by the Association of Gene Ontology, which is applicable to all species and defines and describes the functions of genes and proteins. Using the GO database, genes can be classified according to the biological processes they participate in, the components that make up cells, and the molecular functions they perform. So the GO annotation makes it easier for us to understand the biological meaning behind the genes. GO analysis includes three categories: molecular function (MF), biological process (BP), and cellular component (CC). GO analysis was performed using the clusterProfiler package. The adjusted *P*-value < 0.05 was set as the cut-off criteria [15,16].

2.10. Kyoto encyclopedia of genes and genomes (KEGG) pathway analysis

KEGG is a bioinformatics resource for mining significantly altered metabolic pathways enriched in the gene list. The proteins identified were then subjected to metabolic pathway enrichment analysis, which was also conducted in clusterProfiler package according to the instructions from the KEGG Pathway Database, using the formula described previously. The adjusted *P*-value < 0.05 was set as the cut-off criteria. The results of KEGG pathway analysis were visualized in the bioinformatics platform (http://www.bioinformatics.com.cn/) [17,18]. Pathway analysis of identified proteins can enhance the understanding of metabolic capacity, biological information processes and the mechanisms of related diseases.

2.11. Protein-protein interaction (PPI) network analysis

PPI refers to the generation process of protein complex combined with two or more protein molecules non-covalently. The differentially expressed CCl4-related proteins were imported into STRING database (https://string-db.org/) to perform PPI analysis. The String is a database that searches for known protein-protein interactions and predicts protein-protein interactions for 2031 species, and the database contains 9.6 million proteins and 13.8 million protein-protein interactions. It includes experimental data, text mining results from PubMed abstracts, and a combination of other database data, as well as results predicted using bioinformatics methods. STRING aims to place its focus on coverage (applying to thousands of genome-sequenced organisms), on completeness of evidence sources (e.g., including automated text mining) and on usability features (such as customization, enrichment detection and programmatic access). It allows users to log on and make their searches persistent, and it offers online-viewers to facilitate the inspection of the underlying evidence supporting each protein-protein association. In the PPI network, nodes represent the target proteins, while edges represent the predicted or validated interaction between proteins [19].
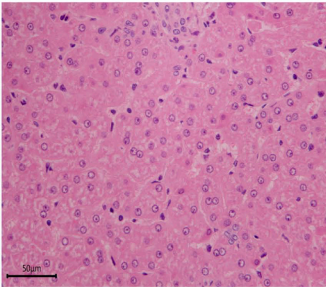
3. Results

3.1. Analysis of biochemistry indexes in serum and the microscope change in liver

Twelve animals (animal No. F7 ∼ F12 and M 7 ∼ M12) used for biochemical indexes determination survived the whole experiment without death. The routine biochemistry indexes of serum showed different change in different time points after CCl4 administration (Fig. 2 A). The serum level of ALT elevated significantly from 24 h after CCl4-induced liver injury, and peaked at 48 h. The top fold change was approximately 57-fold compared with 0 h time point. Unexpectedly, at the 2 h time point, the ALT value decreased slightly and had statistical significance. The AST value began to increase significantly at 4 h after CCl4 administration, peaked at 48 h, then decreased rapidly, and had no statistical significance at 168 h. Although CK began to increase significantly at 2 h and reached its peak at 4 h, it was no longer statistically significant at later time points due to the increase of the standard deviation. Both LDH and TBIL reached statistical significance at 24 h, 48 h and 72 h, and returned to their pre-administration levels at 168 h. As an enzyme marker of liver injury, GGT was the only one that decreased significantly after CCl4 administration and returned to pre-
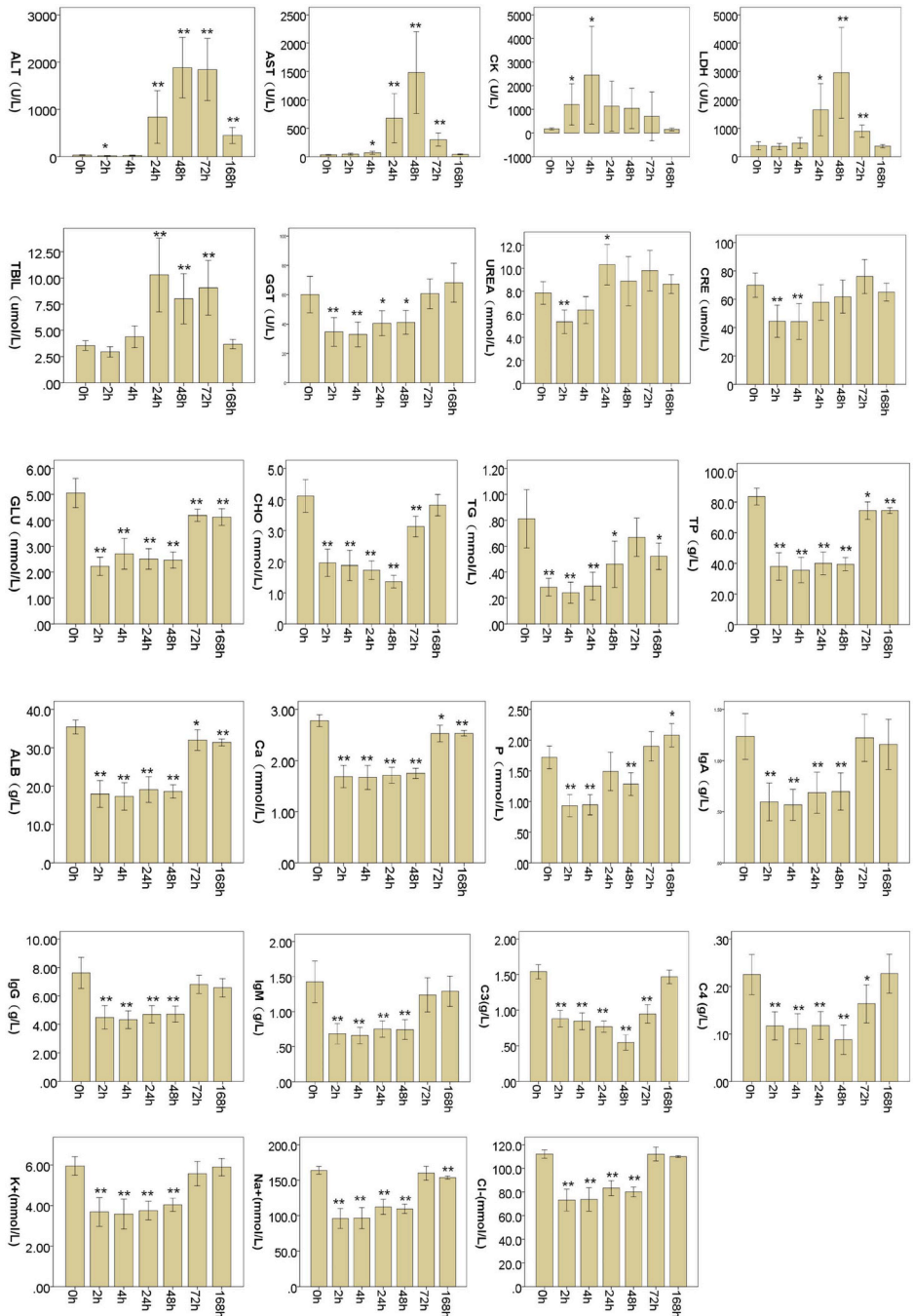
A

B
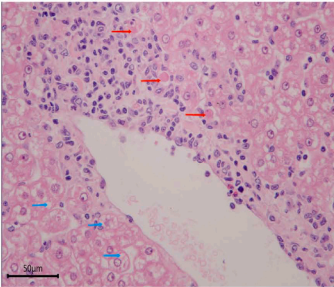
C

(caption on next page)

Fig. 2. The results of biochemistry analysis and microscope examination. The animal No.F7~F12 and M7~M12 were administrated by gavage with 15 % CCl₄ solution (10 mL/kg). Peripheral blood samples were collected before gavage administration, and served as the 0 h blank control samples. Then, peripheral blood samples were collected at 2 h, 4 h, 48 h, 72 h, and 168 h after CCl₄ exposure. (A) Biochemical analysis of all serum was performed. n=12, *P<0.05, **P<0.01. The animal No.F4 was the blank control animal. The animal No.F6 was the positive control animal, which was intoxicated by oral gavage with 15 % CCl₄ solution (10 mL/kg). Liver tissues collected from F4 (B) and F6 (C) at 48 h were examined by microscope. Necrosis (the red arrows) and vacuolation (the blue arrows) of hepatocytes were seen in the CCl₄-relative liver tissue. HE stain, ×40.

---

administration levels at 72 h. UREA and CRE, as markers of renal injury, showed a transient decrease at 2 h after administration. Then, at 4 or 24 h, it returned to its pre-administration level. The value of GLU, CHO, TG, TP, ALB, Ca, and P decreased rapidly at 2 h after CCl₄ administration and began to show a recovery trend at 72 h, with the whole change trend showing a "U" shape. Except for CHO, which had recovered to pre-administration level at 168 h, all other indexes still showed statistically significant decrease at 168 h. However, the value of P at 168 h was slightly higher than that before administration, and the difference was significant. The five immune indexes (IgG, IgM, IgA, C3 and C4) and electrolytes (K^+, Na^+, and Cl^-) decreased significantly at 2 h after administration, and returned to their pre-treatment levels at 72 h or 168 h after administration.

As a marker of liver injury, ALP did not change significantly at all time points after CCl₄ administration, but GGT decreased significantly at 2 h, 4 h, 24 h and 48 h. Although vacuolation and necrosis of hepatocytes had been detected by microscopy at 48 h, GGT still showed a significant reduction compared with 0 h. At 48 h time point after CCl₄ administration, compared with blank control animal (Animal No. F4, Fig. 2B), liver cells in CCl₄-treated animal (15 % CCl₄, 10 mL/kg, Animal No. F6, Fig. 2C) showed necrosis and vacuolation histopathologically. Multifocal necrosis of hepatocytes, nucleolus disappearance of hepatocytes, nuclear collapse and shrinkage, eosinophilic cytoplasm is indicated by red arrow in Fig. 2C. There's a lot of inflammatory cells around, including eosinophil granulocyte. Diffuse vacuolar degeneration of hepatocytes is indicated by the blue arrow. There are a number of different sizes, round and loose light-stained vacuoles in the cytoplasm.

3.2. Quality evaluation of low-abundance proteins extracted and peptides enzymatically hydrolyzed

There are many kinds of proteins in serum, including high-abundance proteins and low-abundance proteins. Among them, low-abundance proteins contain specific markers for disease diagnosis, indicators of disease stage and therapeutic efficacy, and targets of new drugs. In the present study, high abundance proteins were removed and then the proteins were identified by electrophoresis. The result showed that the bands were clear and the concentration was enough to satisfy

the following protein experiment (Fig. 3A). Then enzymatic hydrolysis of the proteins was performed using trypsin and the following steps were performed according to the follow the flowchart in Fig. 1. In the whole scanning range, the peptide mass number deviation was small and relatively stable, indicating the high quality accuracy of the instrument, as well as good stability (Fig. 3B). The ion score of identified peptide indicated good peptide map matching quality (Fig. 3C)

3.3. Identification of differential proteins

A total of 832 proteins with unique peptides or polypeptide segments were identified from all the four isolates (0 h, 2 h, 48 h, and 72 h) by the iTRAQ LC-MS/MS analysis, and a total of 38,090 characteristic peaks were identified (Table 2). Compared with the blank control group, in the 2 h, 48 h, and 72 h time point, 41, 256, and 84 proteins were significantly up-regulated, respectively, and 14, 67, and 74 proteins were significantly down-regulated, respectively (Table 3).

The graph shows the proportion of proteins with different coverage ranges, with different colors representing different sequence coverage ranges. The number of proteins with different coverage ranges and their proportion to the total number of proteins are shown in parentheses in the graph (Fig. 4 A).

The graph shows the distribution of the number of peptides in the identified proteins, with the number of peptides covering the protein in horizontal coordinates and the number of proteins in vertical coordinates. The trends shown in the figure indicate that most of the identified proteins contain fewer than 25 peptides and that the number of proteins decreases as the number of matched peptides increases (Fig. 4B). For each protein, the differential fold distribution is shown below. The up-regulated protein was on the right side of the 1-axis, and the down-regulated protein was on the left side of the 1-axis. If the amount of the same protein does not change significantly between the

Table 2
Protein identification results.

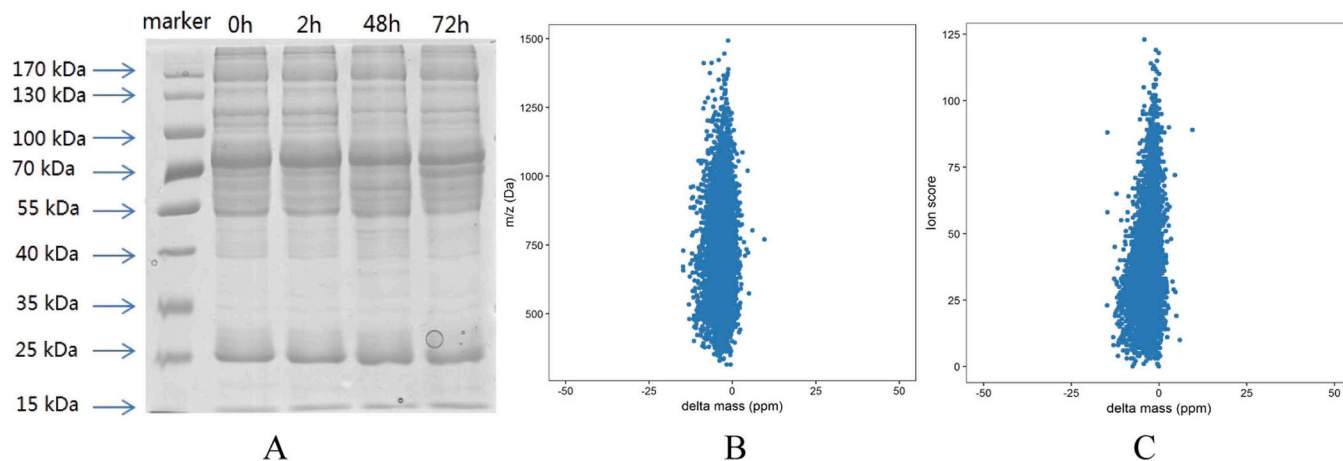| Database spectra (PSM)	Peak	Peptides	Proteins	Quantifiable proteins
Macaque Uniprot	38,090	6805	871	832

Fig. 3. Quality evaluation of low-abundance proteins extracted and peptides enzymatically hydrolyzed, (A) The electrophoretic diagram of the protein. (B) Deviation plot of peptide mass number. (C) Peptide ion score diagram.

Table 3

Differential proteins identified at different time points.

Time point	Up-regulation	Down-regulation
2 h vs. 0 h	41	14
48 h vs. 0 h	256	67
72 h vs. 0 h	84	74

Note: Sample at each time point represents a mixture of six females and six males.

two samples, then the protein abundance ratio is close to 1 (Fig. 4C).

Volcano plots of protein comparison at different time points were showed in Fig. 4 D~F. Abscissa was $\log_{10}$ (Ratio), ordinate was the - $\log_{10}$ (FDR). Red dots represent significant difference proteins.

Significant difference proteins were used for cluster analysis (Fig. 4G). Different columns represent different samples and different rows represent different proteins. The color represents the level of protein expression in the sample. The corresponding protein list for

different clusters was shown in Table 4. Proteins in the same cluster have similar expression patterns and usually have similar biological functions.

3.4. GO and KEGG enrichment analysis of differential proteins

The 3 significant GO genes and 22 signal pathways with the criterion of a *P*-adjust value <0.05 were identified (Table 5). Among the up-regulated differential proteins, significant enrichment focused on KEGG signal pathway. At 48 h, the differential proteins mainly enriched in biosynthesis of antibiotics, biosynthesis of amino acids, and carbon metabolism. At 72 h, the differential proteins enriched in biosynthesis of antibiotics and carbon metabolism. The down-regulated differential proteins mainly happened at 48 h and mainly enriched in CC and KEGG. CC was mainly enriched in extracellular region, extracellular space, and extracellular region part. KEGG was enriched in pertussis, complement and coagulation cascades, and Staphylococcus aureus infection. The differential proteins at 2 h had no GO and KEGG enrichment, and the
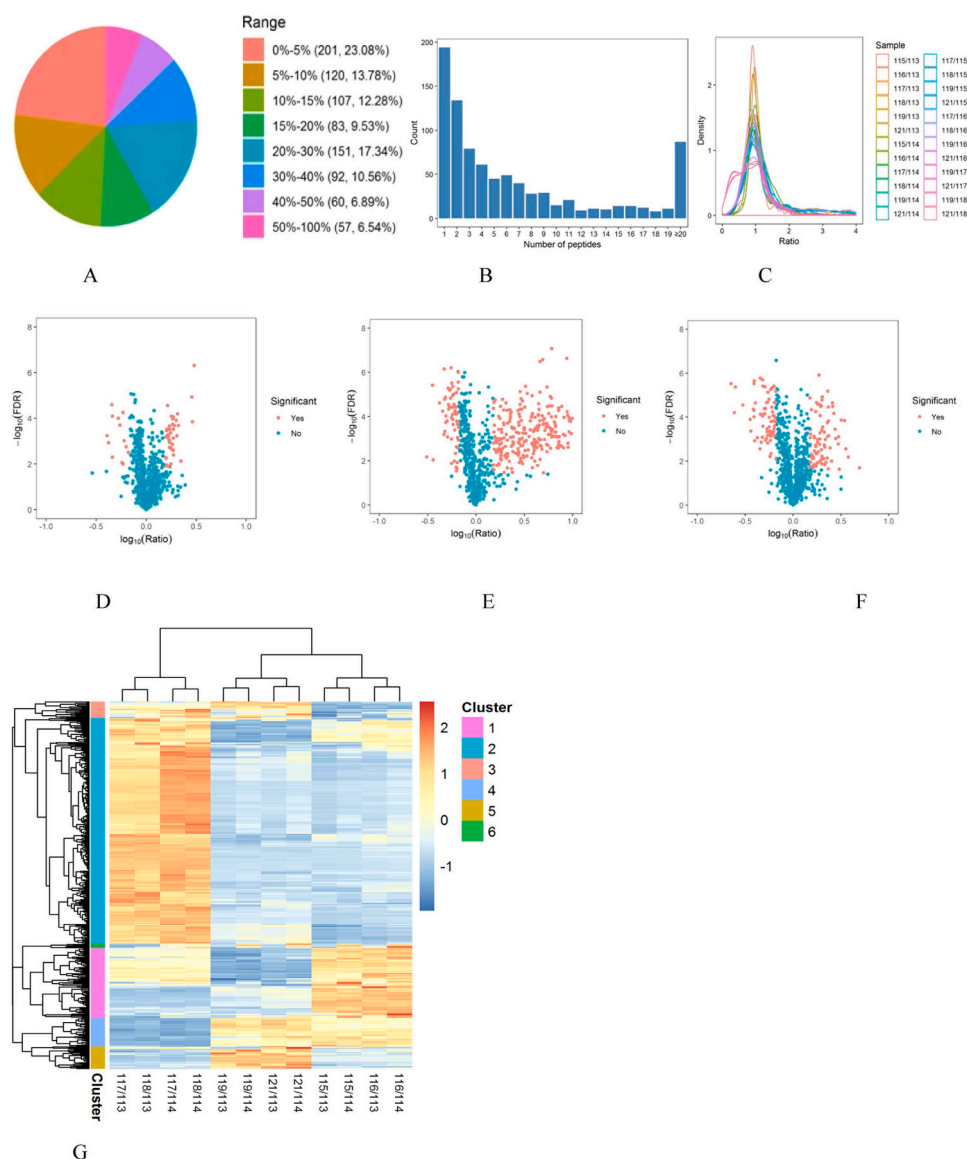

Fig. 4. Identification results of differential proteins, Sample at each time point represent a mixture of six females and six males. (A) Range of Peptide sequence coverage. (B) Distribution of Peptide number. (C) Protein abundance ratio. (D~F) Volcano plots of the differentially expressed CCl$_4$-related proteins at different time points. The red dots in the figure are the proteins with significant difference (*P*<0.05) and the green dots are the proteins with no difference. Compared with 0 h, (D) proteins comparison volcano plot at 2 h, (E) proteins comparison volcano plot at 48 h, (F) proteins comparison volcano plot at 72 h. (G) Cluster analysis of significantly different proteins.

Table 4

Corresponding protein list for different clusters.

Cluster	Proteins accession
1	A0A2K5U1W6,A0A2K5TY33,Q4R6W8,A0A2K5UQC3,A0A2K5VRV3, G8F4W7,G7PEZ9,G7PB85,A0A2K5VUF7,G7P478,G7PHZ9, A0A2K5WE66,Q28911,A0A2K5U150,A0A2K5V3X3,S4UCH4,Q4R5M1, A0A2K5UZY5,A0A2K5X560,A0A2K5UMV4,A0A2K5W2C4, A0A2K5WHA8,A0A2K5UE35,A0A2K5UQZ5,A0A2K5UYN7,A0A2K5X1I0, A0A2K5VFZ7,A0A2K5VHV5,A0A2K5UMM8,G8F6G4,A0A2K5U9F8, A0A2K5UBE7,A0A2K5UJ92,G8F424,I7G3T2,A0A2K5V4F1,G7PJR6, A0A2K5UKJ5,A0A2K5UJW6,G7PTA0,I7GH00,A0A2K5TVM5, A0A2K5TSB3,Q6XMN2,A0A2K5W5U1,G7PZ60,G7PZ61,A0A023JCR5, G7P5M3,A0A2K5UXU0,G7PHA8,A0A2K5U8C7,A0A2K5VGA4, A0A2K5WMT0,A0A2K5V619,A0A2K5WCZ4,A0A2K5WZ65,P68367, A0A2K5VCN4,G7Q0W5,A0A2K5UZY9,A0A2K5W0K9,G7NYM1, A0A2K5WU43,A0A2K5VWV3,A0A2K5VPN1,A0A2K5VU17, A0A2K5WV46,A0A2K5W7D3,G7PJC0,A0A2K5W2A6,A0A2K5W8G8, G7P6S7,A0A2K5UU71,A0A2K5VBQ7,A0A2K5TZC4,A0A2K5UWP1, G7PMA7,A0A2K5WGG1,A0A2K5UIZ0
2	A0A2K5WVF4,A0A2K5WW31,A0A2K5V8G4,A0A2K5V9Y0, A0A2K5UWG3,A0A172R2H3,A0A172R2F8,A0A2K5TP79,A0A2K5X7U5, G7PN12,A0A2K5UG10,A0A172R2H5,A0A2K5UI20,A0A2K5W1V0, G8F6B4,A0A2K5TSE7,A0A2K5V1P3,A0A2K5WCF2,A0A2K5UI29, A0A2K5UQY1,A0A2K5TYP0,A0A2K5UF05,A0A2K5UIQ5,G7PN19, A0A2K5UJE4,G8F4T5,A0A2K5TSL1,A0A2K5UMT9,A0A2K5U4X5, I7GJA1,A0A2K5X592,G7PLQ1,A0A2K5U2R5,A0A2K5UXN7, A0A2K5TK27,G7NZC8,A0A2K5VRI5,A0A2K5WBE9,A0A2K5WLE6, A0A2K5WGG5,I7GH01,A0A2K5TZW4,A0A2K5ULV1,A0A2K5UIV5, Q6LDD9,A0A2K5VGR8,A0A2K5WNF9,A0A2K5VUT8,A0A2K5WLS0, A0A2K5W990,A0A2K5TTJ3,A0A2K5V8G9,A0A2K5V7N6,A0A2K5X7V5, G7PQF0,A0A2K5V9T2,A0A2K5X367,A0A2K5X9B7,A0A2K5VI44, Q60HH3,A0A2K5WMP9,G7PRM2,A0A2K5X1Q8,A0A2K5U3A1, A0A2K5VWZ4,A0A2K5W2M9,A0A2K5UJ46,Q4R568,A0A2K5TJ90, A0A2K5UP92,G7P987,A0A2K5TUG6,G7NYF5,A0A2K5X424,Q4R7X1, A0A2K5VMF6,A0A2K5W5E6,I7GMI4,A0A2K5TVT9,A0A2K5WZH5, A0A2K5UHY6,A0A2K5UD22,A0A2K5WN23,A0A0A7KUP9, A0A2K5UNB1,A0A2K5X4V5,C0SJM2,A0A2K5TPE2,A0A2K5UVB1, A0A2K5UDS4,A0A2K5V6Y0,I7G666,A0A2K5TL96,A0A2K5VUI7,G7PS61, A0A2K5U0R4,Q2PG24,A0A2K5WMN9,G7PIA0,A0A2K5U3W6,Q4R559, A0A2K5VC98,A0A2K5WHN6,Q5IST7,A0A2K5W9M9,C0SJM5,I7GK91, G7PL55,A0A2K5VXA9,A0A2K5WQU0,G7PSJ5,I7G9S0,A0A2K5VK62, Q8HXP3,A0A2K5WXW9,A0A2K5TVN7,G7PGY2,A0A2K5WFJ5, A0A2K5WG48,A0A2K5UTB9,A0A2K5UE39,A0A2K5U1I3,A0A2K5W8T2, I7G8Z1,A0A2K5WKB0,A0A2K5WPZ6,A0A2K5UDS8,A0A2K5VUE2, A0A2K5UZ59,G7NV22,G7P8A8,A0A2K5WZM4,A0A2K5X0E2, A0A2K5TWT3,A0A2K5V8R9,G8F425,A0A2K5X5D0,A0A2K5WQ51, A0A2K5UKE4,A0A172R2G8,A0A2K5UTI1,A0A2K5UNB0,A0A2K5VCB9, A0A2K5UYD5,A0A2K5VKV4,A0A2K5UPF1,A0A2K5VQR3,A0A2K5V7S5, A0A2K5VUD1,A0A2K5W0Z6,G7PY48,A0A2K5VYS2,A0A2K5W4B9, A0A2K5W4P6,G7PT54,G7P4V8,Q4R639,A0A2K5TSB5,A0A2K5V408, A0A2K5WCM9,G7PJX7,A0A2K5TMZ2,I7G8U9,A0A2K5USH8, A0A2K5WAZ7,A0A2K5X7M7,Q4R362,G7PTC0,Q4R520,A0A2K5U1P3, A0A2K5WJA5,A0A2K5W677,A0A2K5X7W4,G7PR80,G7P7U0, A0A171P0Z8,Q4R5L3,A0A2K5UGN6,A0A2K5UXF0,Q9BE95, A0A2K5WX85,A0A2K5WGY6,Q5KTI6,Q4R924,Q4R5U3,A0A2K5UBM3, Q2PG05,G7Q3N8,A0A2K5VVZ6,A0A2K5WFB8,A0A2K5UKM0, A0A2K5VAH7,I7GM66,A0A2K5TUD6,G8F3U9,A0A2K5VZ16,G7P407, A0A2K5UD35,A0A2K5WH26,I7GJY5,A0A2K5UV73,G7Q2J5, A0A2K5WKV0,Q4R4U9,A0A2K5TY35,A0A2K5VMC7,A0A2K5W2M4, G7PJ36,A0A171P0Z3,A0A2K5U618,A0A2K5W7F4,A0A2K5UKL6, G7NW03,A0A2K5U3H0,A0A2K5WV25,A0A2K5VR14,A0A2K5VQT4, A0A2K5VBL1,A0A2K5WN93,A0A2K5W2Y6,A0A2K5VJL2,A0A2K5V8H3, A0A2K5WX26,A0A2K5V5J5,A0A2K5WN81,G7PEX6,A0A2K5W6A0, G8F2N9,A0A2K5UV66,A0A2K5U9B0,A0A2K5UMB6,A0A2K5WTC0, A0A2K5VR98,G7NWZ5,A0A2K5VIT7,A0A2K5UVM6,A0A2K5UW57, A0A2K5WT45,G7NX69,G7PRG1,A0A2K5VCV5,A0A2K5TU04, A0A2K5W3X6,A0A2K5TUD6,G7NXX6,G7PRL2,I7G2Y1,A0A2K5VHI3, A0A2K5W387,A0A2K5TJQ4,A0A2K5U9Z7,A0A2K5VHT3,A0A2K5VX98, A0A2K5VN00,A0A2K5WU34,A0A2K5W9Z6,G7P9U7,A0A2K5U0M7, A0A2K5V990,G7PGJ4,A0A2K5V886,I7G9D1
3	G7PHT9,A0A2K5VSR8,A2V9Z3,A0A2K5VRF5,A0A2K5VRQ2,G7PBE4, A0A2K5UEU7,G7P6F9,A0A2K5VSD9,A0A2K5TZD7,A0A2K5U224, A0A2K5UJN7,A0A2K5WMU8,Q4R4X6,A0A2K5VKZ4,A0A2K5UE84, A0A2K5V5N6,A0A2K5VUN3,G7PFM1
4	G8F3V9,G7PQY3,G7P3F6,G7PVR8,A0A2K5WEE7,P18657,A0A2K5VPK0, A0A2K5VV99,Q2PFZ3,A0A2K5WIF5,G7PDZ7,G7PP12,A0A2K5VQK4, A0A2K5VHK1,A0A2K5W172,A0A2K5V1A0,A0A2K5WAC5,G7PQA7,

Table 4 (*continued*)

Cluster	Proteins accession
	A0A2K5WNU6,A0A2K5VA60,G7PBE3,G7PXX2,G7P4B6,A0A2K5V1A1, A0A2K5V7N8,A0A2K5VUU4,G7NWI5,A0A2K5TU41,A0A2K5U480, A0A2K5TJJ6,A0A2K5VPR7,A0A2K5UTP0,G8F3W0
5	P68109,A0A2K5VCN7,G7P0L2,A0A2K5UDH3,G7PEY1,A0A2K5TWX6, A0A2K5WY01,A0A2K5UET1,A0A2K5WH09,I7GH44,A0A2K5VXG2, G7PDL6,A2V9Y5,G7P5L7,G7PJP4,A0A2K5WIV2,A2V9Z4,G7PC54, A0A2K5U6K3,G7PLD4,A0A2K5UK15,A0A2K5TP96,A0A2K5V4R6, A0A2K5TYM1,A0A2K5UDF7,A0A2K5VRD0
6	G7P4A8,A0A2K5UV59,A0A2K5VXR0,A0A2K5UIH5,A0A2K5WWX2

differential proteins at 72 h had no GO enrichment, because the number of differential proteins at the two time points was too small.

3.5. PPI analysis of differential proteins

PPI analysis was performed to determine the interactions among differentially expressed CCl_4-related proteins using STRING database. A PPI network of differential proteins at 2 h that included 3 nodes and 2 edges was constructed to identify protein interactions, as shown in Fig. 5A. There were 52 nodes and 91 edges, 13 nodes and 10 edges in the PPI network of differential proteins at 48 h, and 72 h, respectively (Fig. 5B and C).

4. Discussion

The model of CCl_4-induced liver injury is a classical model to discover the effect and mechanism of drugs on liver. Generally, it is considered that CCl_4 induces liver injury through activating hepatic microsomal cytochrome P450 (CYP) enzymes, phase I drug metabolism, or detoxification enzymes to produce CCl_3 and CCl_3O_2 free radicals. The liver has an endogenous antioxidant enzyme system such as GSH, glutathione-s-transferase (GST), catalase and sulphuroxide dismutase (SOD). These antioxidants are induced by hepatocytes to combat oxidative stress. However, when the oxidative stress increases beyond the neutralizing capacity, the liver is the most vulnerable tissue for the free radicals related damage. These free radicals could interact directly or indirectly with nucleic acids, proteins, lipids, and carbohydrates, attacking unsaturated lipids under the cell membrane to induce lipid peroxidation (LPO). LPO and its degradation products may also impair the stability and integrity of various biofilms and increase their permeability, leading to the release of enzymes and cytokines from the cytoplasm into the blood, such as ALT, AST, IL-1β, IL-6, and TNF-α [20]. Cytokines released by cells can promote inflammation and further induce apoptosis and necrosis of cells.

Non-human primates are genetically similar to human and are thought to have the most similar toxic mechanisms. In current study, *Macaca fascicularis* were administrated with CCl_4 to construct the liver injury animal model. CCl_4 was diluted to 15 % using peanut oil , and was administrated at a dose of 10 mL/kg. Pathological examination of liver tissue at 48 h after CCl_4 administration showed vacuolation or necrosis of hepatocytes, which proved that liver injury had occurred at 48 hours. Comprehensive biochemical tests were performed including routine biochemical indexes and immunological parameters. The value of ALT elevated significantly from 24 h after CCl_4-induced liver injury, and peaked at 48 h. Subsequently, the ALT value decreased gradually in time-dependent manner, but the difference was still statistically significant compared with 0 h. As a specific biomarker of liver injury, ALT showed a typical time-effect curve. Unexpectedly, at the 2 h time point, the ALT value decreased slightly and had statistical significance. The significant decrease of ALT at 2 h seems to be related to the stress response after CCl_4 stimulation, but the specific mechanism is still unclear. As another classical biomarker of liver injury, AST increased significantly at 4 h and peaked at 48 h. Subsequently, it decreased rapidly, and there was no significant difference at 168 h compared with

Table 5

Significantly enriched GO and KEGG of differential proteins in different time points.

| Cluster	Category	ID	Description	P-adjust	Count	Protein symbol
upregulated						
48 h	KEGG	mcf01130	Biosynthesis of antibiotics	2.42E−11	23	ALDOB,PCK2,MDH2,OTC,UGP2,ARG1,AADAT,IDH1,CAT,PCK1,PCCA, SHMT1,GAPDH,CTH,GOT2,HMGCS2
48 h	KEGG	mcf01230	Biosynthesis of amino acids	2.69E−08	13	ALDOB,IDH1,CPS1,MAT2A,PAH,OTC,SHMT1,CTH,GAPDH,ARG1,GOT2
48 h	KEGG	mcf01200	Carbon metabolism	4.35E−07	14	ALDOB,CPS1,MDH2,IDH1,CAT,TKFC,PCCA,SHMT1,GAPDH,GOT2
48 h	KEGG	mcf00260	Glycine, serine and threonine metabolism	4.36E−05	8	BHMT,DMGDH,GNMT,SARDH,SHMT1,CTH,GRHPR
48 h	KEGG	mcf00220	Arginine biosynthesis	0.000190342	6	CPS1,OTC,ARG1,GOT2
48 h	KEGG	mcf04146	Peroxisome	0.00031517	9	IDH1,CAT,ACOX2,SOD2,ACSL1,BAAT,XDH,EPHX2
48 h	KEGG	mcf00270	Cysteine and methionine metabolism	0.000390642	7	BHMT,MAT2A,MDH2,CTH,GOT2
48 h	KEGG	mcf00630	Glyoxylate and dicarboxylate metabolism	0.000629925	6	CAT,PCCA,SHMT1,MDH2,GRHPR
48 h	KEGG	mcf00983	Drug metabolism - other enzymes	0.002646747	6	TYMP,DPYS,CDA,HPRT1,XDH,UPB1
48 h	KEGG	mcf00071	Fatty acid degradation	0.003024606	6	ACSL1,ECI1,ADH4
48 h	KEGG	mcf00620	Pyruvate metabolism	0.005145569	6	PCK1,PCK2,MDH2,GRHPR
48 h	KEGG	mcf00280	Valine, leucine and isoleucine degradation	0.006843382	6	PCCA,HMGCS2
48 h	KEGG	mcf00480	Glutathione metabolism	0.006928434	6	IDH1,GSTO1,LAP3,GSTM5,GSR,GCLC
48 h	KEGG	mcf00350	Tyrosine metabolism	0.015121448	5	HGD,HPD,FAH,GOT2,ADH4
48 h	KEGG	mcf03320	PPAR signaling pathway	0.018266211	6	PCK1,FABP1,ACOX2,PCK2,ACSL1
48 h	KEGG	mcf03050	Proteasome	0.028593456	5	PSMB3,PSMA5,PSMA7,PSMB1
48 h	KEGG	mcf00010	Glycolysis, Gluconeogenesis	0.034098099	6	ALDOB,PCK1,PCK2,GAPDH,ADH4
72 h	KEGG	mcf01130	Biosynthesis of antibiotics	0.004713028	7	ALDOB,PCK1,PCCA,UGP2
72 h	KEGG	mcf01200	Carbon metabolism	0.02133288	5	ALDOB,PCCA
downregulated						
48 h	CC	GO:0005576	Extracellular region	0.000204049	7	ALB,SERPIND1,FETUB,APOC2,APOC1B,GC
48 h	CC	GO:0005615	Extracellular space	0.000634237	5	ALB,SERPIND1,FETUB,APOC2,GC
48 h	CC	GO:0044421	Extracellular region part	0.000803342	5	ALB,SERPIND1,FETUB,APOC2,GC
48 h	KEGG	mcf05133	Pertussis	0.043169203	3	C3
48 h	KEGG	mcf04610	Complement and coagulation cascades	4.85E−07	6	F10,SERPIND1,PLG,C3
48 h	KEGG	mcf05150	Staphylococcus aureus infection	0.000638608	4	PLG,C3
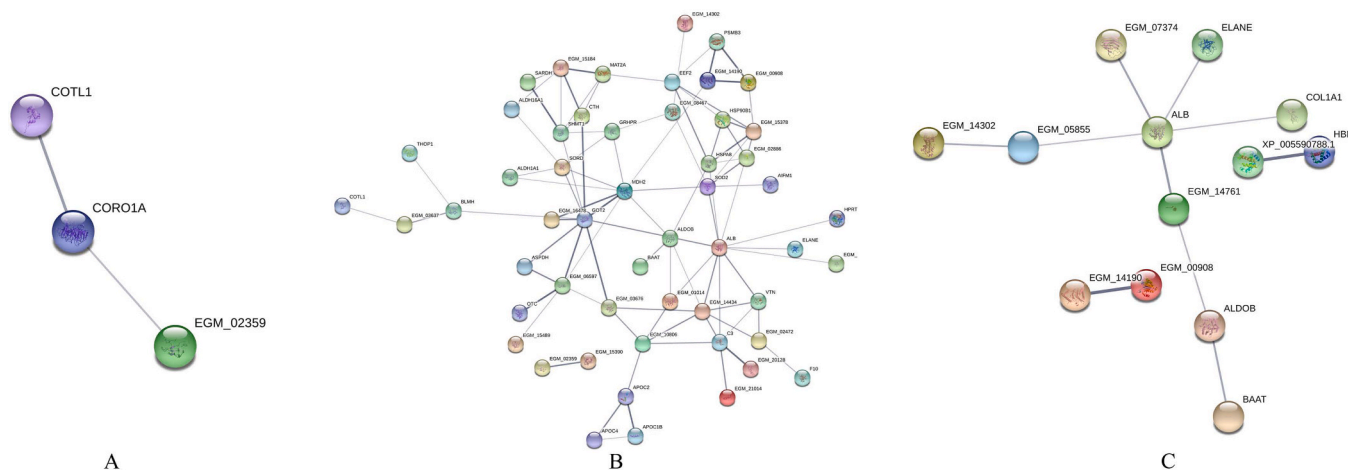
Fig. 5. The PPI network of differential proteins in different time points Sample at each time point represent a mixture of six females and six males. (A) Interaction network of differentially expressed proteins in 2 h_vs_0h group. (B) Interaction network of differentially expressed proteins in 48 h_vs_0h group. (C) Interaction network of differentially expressed proteins in 72 h_vs_0h group. In the protein interaction network, nodes represent proteins, lines represent the interactions between proteins, and results inside the circle represent protein structure.

0 h. CK showed a good sensitivity, which increased significantly at 2 h and reached a peak at 4 h. However, due to the large individual differences caused by its poor specificity, CK showed no significant difference from 24 h.

LDH and TBIL showed similar increase at 24 h, 48 h and 72 h, and recovered to the pre-dose level at 168 h. LDH and TBIL have some diagnostic value for liver injury caused by CCl₄. The changes of ALP and GGT after CCl₄ administration were different from that of other liver enzyme indexes. The increase of GGT was generally found in the damage of biliary system, including the damage of extrahepatic biliary system

and intrahepatic bile duct, autoimmune liver disease and viral liver injury. In the current study, GGT was the only one enzyme biomarker that decreased significantly after CCl₄ administration and returned to pre-administration levels at 72 h. ALP, an important biomarker of intrahepatic cholestasis and obstructive jaundice, did not show any significant changes after administration of CCl₄ in this study, which was consistent with the characteristics of acute liver injury. Additionally, a transient decrease of UREA, CRE, GLU, CHO, TG, TP, ALB, Ca, P, IgG, IgM, IgA, C3, C4, K$^+$, Na$^+$, and Cl$^-$ occurred at 2 h after CCl₄ administration, which may result from a reaction with free radicals produced in

vivo. These parameters gradually returned to or approached their pre-administration levels at subsequent time points, which may be related to reduced CCl$_4$ content, attenuated toxicity, or feedback mechanisms of body protection.

According to the changes of serum biochemical indexes and liver histopathology after CCl$_4$ administration, the serum samples at 0 h, 2 h, 48 h and 72 h were selected for the iTRAQ analysis. iTRAQ is a powerful technique for the identification of differentially expressed proteins, which was established by Applied Biosystems Incorporation. Generally, the extracted proteins were hydrolyzed by enzyme, then the 8-plex iTRAQ reagent was used to label the hydrolyzed peptides, then the mass spectrometry analysis was performed. In tandem mass spectrometry, the same polypeptide with different isotope tags produced different reporter ions, the quantitative information of the same peptide can be obtained from the reported ion signal intensity, and then the quantitative information of protein can be obtained by software processing [21]. In the present study, the results showed that 832 proteins were quantifiable proteins. Compared with 0 h, 55, 323, and 158 differential proteins were detected at 2 h, 48 h, and 72 h, respectively. These differential proteins are the potential biomarkers of stress and toxicity after administration of CCl$_4$ in vivo.

Bioinformatics analysis of GO enrichment revealed that only down-regulated proteins at 48 h showed significant enrichment (adjusted *P*-value < 0.05), and any proteins at other time points showed no significant GO enrichment. These down-regulated differential proteins at 48 h were mainly enriched in cellular components, including the parts of a cell or its extracellular environment. There was no significant enrichment of differential proteins involved in biological processes and molecular functions. This suggests that the main damage at 48 h after CCl$_4$ administration is cellular damage in vivo. At 48 h, KEGG enrichment revealed that these up-regulated and down-regulated proteins showed significant enrichment (adjusted *P*-value < 0.05). The top three signal pathways of KEGG enrichment for up-regulated proteins were biosynthesis of antibiotics, biosynthesis of amino acids, and carbon metabolism, and the results of KEGG enrichment for down-regulated proteins were mainly in pertussis, complement and coagulation cascades, and Staphylococcus aureus infection. The origin of antibiotics biosynthesis was considered to be related with the 'thiotemplate multienzymic mechanism'. This mechanism includes the activation of the constituent residues as adenylates, the acylation of specific template thiol groups, epimerization or N-methylation, and polymerization in the sequence directed by the multienzymic structure with the aid of 4′-phospho-pantetheine as a cofactor [22]. In addition, these highly expressed differential proteins are also involved in amino acid biosynthesis and carbon metabolism, which may be a toxic effect after CCl$_4$ administration, or may also be a protective feedback against toxic effects.

Proteins down-regulated involved in the signaling pathway is mainly related to the activation of natural immune signals. The down-regulation of related proteins leads to the attenuation of the activation of immune pathway, which confirms the inhibition of CCl$_4$ on immune response in vivo. At 72 h, antibiotic biosynthesis and carbon metabolism were the significantly enriched signal pathways using KEGG analysis, and these two metabolic pathways were also significantly enriched at 48 h. These suggest that differential proteins involved in biosynthesis and carbon metabolism, which persist after CCl$_4$ administration, are candidates for biomarkers of toxicity.

PPI and the obtained networks are very important in the majority of biological functions and processes, while most of the proteins appear to activate their functionalities through their interaction [23]. Network of PPI and key function with their related targets were performed and the degree of network was calculated with Cytoscape. In the present study, the key interaction node proteins after CCl$_4$ treatment were 3, 52, and 13 at 2 h, 48 h and 72 h, respectively. We reported that, at 48 h and 72 h, common nodal protein-coding genes were included ALB, ALDOB, BAAT, EGM-00908, EGM-14190, EGM-14302, and ELANE, which encoded serum ALB, enzyme aldolase B, bile acid-CoA: amino acid

N-acyltransferase, proteasome subunit alpha type (EC 3.4.25.1), proteasome subunit beta (EC 3.4.25.1), UDP-glucose 6-dehydrogenase (UGDH)(EC 1.1.1.22), and neutrophil elastase (NE), respectively. Aldolase B (ALDOB) is a glycolytic enzyme and plays a contentious role in cancers progress. It was reported that ALDOB can either act against the tumor or as an oncogenic enzyme. Particularly, metastatic cells in the liver could upregulate the enzyme ALDOB via GATA6, which could enhance fructose metabolism and provide fuel for major pathways of central carbon metabolism during tumor cell proliferation [24,25]. Bile acid CoA: amino acid N-acyltransferase (BAAT) is the terminal enzyme in the synthesis of bile salts from cholesterol. It could catalyze the conjugation of taurine or glycine to bile acid CoA thioesters to form bile acid N-acylamidates [26]. Proteasomes are the essential components of complexes involved in an extralysosomal energy- and ubiquitin-dependent proteolytic pathway. It is reported that the transcripts of both the alpha-type and beta-type proteasome subunits in cells accumulate to high levels during cell proliferation , which suggest that proteasomes in cells may be involved in the progression of the cell cycle [27]. The UGDH produces UDP-α-D-glucuronic acid, a precursor of extracellular matrix glycosaminoglycans (GAGs) and proteoglycans. Elevated GAG formation has been associated with a variety of human diseases, including glioblastoma (GBM) [28]. Additionally, it was reported that UGDH could regulate hyaluronic acid production and promote breast cancer progression. It is considered that inhibition of synthesis of the hyaluronan precursor UDP-glucuronic acid therefore presents an emerging target for cancer therapy [29]. The NE, a major inflammatory protease released by neutrophils, is present in the airways of patients with cystic fibrosis (CF), chronic obstructive pulmonary disease, non-CF bronchiectasis, and bronchopulmonary dysplasia. Although NE promotes the migration of white blood cells to the site of infection and is required for Gram-negative clearance, it also activates inflammation when released into the airway environment in chronic inflammatory airway disease. Neutrophil elastase is not only a factor mediating lung inflammation, but also an important factor in other diseases and is a potential therapeutic target [30].

There is still much to be done in this experiment. For example, we can use the electron microscope to study the ultrastructural changes of hepatocytes after CCl$_4$ hepatotoxicity. We can study the dose-dependent toxicity of different levels of CCl$_4$ and the changes of gene expression profiling in peripheral blood in *Macaca fascicularis*. Proteomic differences between the CCl$_4$ model and other hepatotoxicity models can also be further studied. Nevertheless, this study has demonstrated that the toxicological mechanism of CCl$_4$ hepatotoxicity was related to a variety of biological processes, pathways and targets, and can provide new target selection for clinical treatment of liver diseases.

5. Conclusion

Our proteomic analysis identified a number of key differential proteins that warrant further investigation as potential new biomarkers of CCl$_4$ toxicity. Bioinformatics analysis showed that multiple signaling pathways were involved in the development of CCl$_4$ toxicity and potential protection reaction of CCl$_4$ detoxication.

Author Statement

Miao Yufa declares that he has no conflict of interest.
Chen Dongmei declares that she has no conflict of interest.
Li Wei declares that he has no conflict of interest.
Li Shuangxing declares that she has no conflict of interest.
Sun Li declares that she has no conflict of interest.
Geng Xingchao declares that he has no conflict of interest.
Both Miao Yufa and Chen Dongmei contributed equally.

All applicable international,national,and institutional guidelines for the care and use of animals were followed.

This article does not contain any studies with human participants performed by any of the authors.

CRediT authorship contribution statement

Miao Yufa: Writing – original draft. **Chen Dongmei:** Writing – review & editing, Formal analysis. **Li Wei:** Writing – review & editing. **Li Shuangxing:** Resources, Data curation. **Sun Li:** Resources, Investigation, Formal analysis. **Geng Xingchao:** Project administration, Funding acquisition.

Declaration of Competing Interest

The authors declare that they have no known competing financial interests or personal relationships that could have appeared to influence the work reported in this paper.

Data availability

Data will be made available on request.

References

[1] D. Frank, S. Savir, B.F. Gruenbaum, I. Melamed, J. Grinshpun, R. Kuts, B. Knyazer, A. Zlotnik, M. Vinokur, M. Boyko, Inducing acute liver injury in rats via carbon tetrachloride (CCl4) exposure through an orogastric tube, J. Vis. Exp. (158) (2020), https://doi.org/10.3791/60695. PMID: 32420997; PMCID: PMC7859859.

[2] I. Naz, M.R. Khan, J.A. Zai, R. Batool, Z. Zahra, A. Tahir, Pilea umbrosa ameliorate CCl₄ induced hepatic injuries by regulating endoplasmic reticulum stress, pro-inflammatory and fibrosis genes in rat, Environ. Health Prev. Med. 25 (1) (2020) 53, https://doi.org/10.1186/s12199-020-00893-2. PMID: 32917140; PMCID: PMC7488709.

[3] J.Q. Zhang, L. Shi, X.N. Xu, S.C. Huang, B. Lu, L.L. Ji, Z.T. Wang, Therapeutic detoxification of quercetin against carbon tetrachloride-induced acute liver injury in mice and its mechanism, J. Zhejiang Univ. Sci. B 15 (12) (2014) 1039–1047, https://doi.org/10.1631/jzus.B1400104. PMID: 25471833; PMCID: PMC4265558.

[4] M. Ebeling, E. Küng, A. See, C. Broger, G. Steiner, M. Berrera, T. Heckel, L. Iniguez, T. Albert, R. Schmucki, H. Biller, T. Singer, U. Certa, Genome-based analysis of the nonhuman primate Macaca fascicularis as a model for drug safety assessment, Genome Res. 21 (10) (2011) 1746–1756, https://doi.org/10.1101/gr.123117.111. Epub 2011 Aug 23. PMID: 21862625; PMCID: PMC3202291.

[5] G. Weinbauer, L. Mecklenburg, Does geographical origin of long-tailed macaques (*Macaca fascicularis*) matter in drug safety assessment?: A literature review and proposed conclusion, Toxicol. Pathol. 50 (5) (2022) 552–559, https://doi.org/10.1177/01926233221095443. Epub 2022 May 24. PMID: 35608013.

[6] S.C. Qu, D. Xu, T.T. Li, J.F. Zhang, F. Liu, iTRAQ-based proteomics analysis of aqueous humor in patients with dry age-related macular degeneration, Int. J. Ophthalmol. 12 (11) (2019) 1758–1766, https://doi.org/10.18240/ijo.2019.11.15. PMID: 31741866; PMCID: PMC6848880.

[7] S. Dong, Q.L. Chen, Y.N. Song, Y. Sun, B. Wei, X.Y. Li, Y.Y. Hu, P. Liu, S.B. Su, Mechanisms of CCl4-induced liver fibrosis with combined transcriptomic and proteomic analysis. J. Toxicol. Sci. 41 (4) (2016) 561–572, https://doi.org/10.2131/jts.41.561. PMID: 27452039.

[8] L. Tian, H.Z. You, H. Wu, Y. Wei, M. Zheng, L. He, J.Y. Liu, S.Z. Guo, Y. Zhao, R. L. Zhou, X. Hu, iTRAQ-based quantitative proteomic analysis provides insight for molecular mechanism of neuroticism, Clin. Proteom. 16 (2019) 38, https://doi.org/10.1186/s12014-019-9259-8. PMID: 31719821; PMCID: PMC6839193.

[9] Y. Cao, B. Duan, X. Gao, E. Wang, Z. Dong, iTRAQ-based comparative proteomics analysis of urolithiasis rats induced by ethylene glycol, Biomed. Res. Int. 2020 (2020) 6137947, https://doi.org/10.1155/2020/6137947. PMID: 32509863; PMCID: PMC7246402.

[10] R.R.V. Binitha, M.A. Shajahan, J. Muhamed, T.V. Anilkumar, S. Premlal, V. C. Indulekha, Hepatoprotective effect of Lobelia alsinoides Lam. in Wistar rats, J. Ayur. Integr. Med. 11 (4) (2020) 515–521, https://doi.org/10.1016/j.jaim.2019.04.004. Epub 2019 Jul 2. PMID: 31277907; PMCID: PMC7772512.

[11] I.C. Lee, S.H. Kim, H.S. Baek, C. Moon, S.H. Kim, Y.B. Kim, W.K. Yun, H.C. Kim, J. C. Kim, Protective effects of diallyl disulfide on carbon tetrachloride-induced hepatotoxicity through activation of Nrf2, Environ. Toxicol. 30 (5) (2015) 538–548, https://doi.org/10.1002/tox.21930. Epub 2013 Dec 1. PMID: 24293383.

[12] C. Dai, X. Xiao, D. Li, S. Tun, Y. Wang, T. Velkov, S. Tang, Chloroquine ameliorates carbon tetrachloride-induced acute liver injury in mice via the concomitant inhibition of inflammation and induction of apoptosis, Cell Death Dis. 9 (12) (2018) 1164, https://doi.org/10.1038/s41419-018-1136-2. PMID: 30478280; PMCID: PMC6255886.

[13] J.R. Wiśniewski, Quantitative evaluation of filter aided sample preparation (FASP) and multienzyme digestion FASP protocols, Anal. Chem. 88 (10) (2016) 5438–5443, https://doi.org/10.1021/acs.analchem.6b00859. Epub 2016 May 6. PMID: 27119963.

[14] J.H. Chen, L.L. Wang, L. Tao, B. Qi, Y. Wang, Y.J. Guo, L. Miao, Identification of MYH6 as the potential gene for human ischaemic cardiomyopathy, J. Cell Mol. Med. 25 (22) (2021) 10736–10746, https://doi.org/10.1111/jcmm.17015. Epub 2021 Oct 26. PMID: 34697898; PMCID: PMC8581323.

[15] Y. Zhou, C Zhang, Z. Zhou, C. Zhang, J Wang, Identification of key genes and pathways associated with *PIEZO1* in bone-related disease based on bioinformatics, Int. J. Mol. Sci. 23 (9) (2022) 5250, https://doi.org/10.3390/ijms23095250. PMID: 35563641; PMCID: PMC9104149.

[16] S. Sun, Y. Shen, J. Wang, J. Li, J. Cao, J. Zhang, Identification and validation of autophagy-related genes in chronic obstructive pulmonary disease, Int. J. Chron. Obstruct. Pulmon. Dis. 16 (2021) 67–78, https://doi.org/10.2147/COPD.S288428. PMID: 33469280; PMCID: PMC7811454.

[17] Y. Aihaiti, Y. Song Cai, X. Tuerhong, Y. Ni Yang, Y. Ma, H. Shi Zheng, K. Xu, P. Xu, Therapeutic effects of naringin in rheumatoid arthritis: network pharmacology and experimental validation, Front. Pharmacol. 12 (2021) 672054, https://doi.org/10.3389/fphar.2021.672054. PMID: 34054546; PMCID: PMC8160516.

[18] G.M. Li, C.L. Zhang, R.P. Rui, B. Sun, W. Guo, Bioinformatics analysis of common differential genes of coronary artery disease and ischemic cardiomyopathy, Eur. Rev. Med. Pharmacol. Sci. 22 (11) (2018) 3553–3569, https://doi.org/10.26355/eurrev_201806_15182. PMID: 29917210.

[19] D. Szklarczyk, A.L. Gable, K.C. Nastou, D. Lyon, R. Kirsch, S. Pyysalo, N. T. Doncheva, M. Legeay, T. Fang, P. Bork, L.J. Jensen, C. von Mering, The STRING database in 2021: customizable protein-protein networks, and functional characterization of user-uploaded gene/measurement sets, Nucleic Acids Res. 49 (D1) (2021) D605–D612, https://doi.org/10.1093/nar/gkaa1074. PMID: 33237311; PMCID: PMC7779004.

[20] G. Xu, X. Han, G. Yuan, L. An, P. Du, Screening for the protective effect target of deproteinized extract of calf blood and its mechanisms in mice with CCl4-induced acute liver injury, PLOS One 12 (7) (2017) e0180899, https://doi.org/10.1371/journal.pone.0180899. PMID: 28700704; PMCID: PMC5507287.

[21] S. Wiese, K.A. Reidegeld, H.E. Meyer, B. Warscheid, Protein labeling by iTRAQ: a new tool for quantitative mass spectrometry in proteome research, Proteomics 7 (3) (2007) 340–350, https://doi.org/10.1002/pmic.200600422. PMID: 17177251.

[22] H. Kleinkauf, H. von Döhren, Nonribosomal biosynthesis of peptide antibiotics, Eur. J. Biochem. 192 (1) (1990) 1–15, https://doi.org/10.1111/j.1432-1033.1990.tb19188.x. PMID: 2205497.

[23] A. Athanasios, V. Charalampos, T. Vasileios, G.M. Ashraf, Protein-protein interaction (PPI) network: recent advances in drug discovery, Curr. Drug Metab. 18 (1) (2017) 5–10, https://doi.org/10.2174/138920021801170119204832. PMID: 28889796.

[24] C. Peng, X. Yang, X. Li, Z. Ye, J. Wang, W. Wu, ALDOB plays a tumor-suppressive role by inhibiting AKT activation in gastric cancer, J. Cancer 14 (12) (2023) 2255–2262, https://doi.org/10.7150/jca.83456. PMID: 37576390; PMCID: PMC10414037.

[25] P. Bu, K.Y. Chen, K. Xiang, C. Johnson, S.B. Crown, N. Rakhilin, Y. Ai, L. Wang, R. Xi, I. Astapova, Y. Han, J. Li, B.B. Barth, M. Lu, Z. Gao, R. Mines, L. Zhang, M. Herman, D. Hsu, G.F. Zhang, X. Shen, Aldolase B-mediated fructose metabolism drives metabolic reprogramming of colon cancer liver metastasis, Cell Metab. 27 (6) (2018) 1249–1262.e4, https://doi.org/10.1016/j.cmet.2018.04.003. Epub 2018 Apr 26. PMID: 29706565; PMCID: PMC5990465.

[26] N.A. Styles, E.M. Shonsey, J.L. Falany, A.L. Guidry, S. Barnes, C.N. Falany, Carboxy-terminal mutations of bile acid CoA:N-acyltransferase alter activity and substrate specificity, J. Lipid Res. 57 (7) (2016) 1133–1143, https://doi.org/10.1194/jlr.M064428. Epub 2016 May 25. PMID: 27230263; PMCID: PMC4918843.

[27] P. Genschik, E. Jamet, G. Philipps, Y. Parmentier, C. Gigot, J. Fleck, Molecular characterization of a beta-type proteasome subunit from Arabidopsis thaliana co-expressed at a high level with an alpha-type proteasome subunit early in the cell cycle, Plant J. 6 (4) (1994) 537–546, https://doi.org/10.1046/j.1365-313x.1994.6040537.x. PMID: 7987412.

[28] C.R. Goodwin, A.K. Ahmed, S. Xia, UDP-α-D-glucose 6-dehydrogenase: a promising target for glioblastoma, Oncotarget 10 (16) (2019) 1542–1543, https://doi.org/10.18632/oncotarget.26670. PMID: 30899420; PMCID: PMC6422181.

[29] J.M. Arnold, F. Gu, C.R. Ambati, U. Rasaily, E. Ramirez-Pena, R. Joseph, M. Manikkam, R. San Martin, C. Charles, Y. Pan, S.S. Chatterjee, P. Den Hollander, W. Zhang, C. Nagi, A.G. Sikora, D. Rowley, H.X. Zhang, B. Karanam, S. A. Mani, A. Sreekumar, UDP-glucose 6-dehydrogenase regulates hyaluronic acid production and promotes breast cancer progression, Oncogene 39 (15) (2020) 3089–3101, https://doi.org/10.1038/s41388-019-0885-4. PMID: 31308490; PMCID: PMC6960374.

[30] J.A. Voynow, M. Shinbashi, Neutrophil elastase and chronic lung disease, Biomolecules 11 (8) (2021) 1065, https://doi.org/10.3390/biom11081065. PMID: 34439732; PMCID: PMC8394930.